EXPERIMENTS ON SMELT SHATTERING AND DISSOLUTION

Markus Bussmann, Eric Jin, Michael Lin, Andrew Jones and Honghi Tran
University of Toronto
Toronto, Ontario, Canada

ABSTRACT

An effective and safe dissolving tank is key to the proper management of a kraft recovery operation. While dissolving tank explosions that lead to equipment damage, personnel injury, and unscheduled shutdowns are thankfully rare, loud and violent dissolving tank operation is a surprisingly common occurrence at many mills. Such operating conditions are believed to be the result of inadequate shattering, when relatively large clumps of smelt fall into the dissolving tank. This paper presents results of two ongoing studies being conducted at the University of Toronto on smelt shattering and dissolution. 1) A scaled-down experimental apparatus is being used to examine smelt shattering, with water-glycerine solutions and air used in place of smelt and steam. A high-speed camera and an automated image processing methodology are being used to quantify liquid shattering (in terms of droplet size and number distributions) as a function of air and water flow rates, and different air nozzle geometries and positions. The objective is to identify best practices for smelt shattering. 2) A study is underway to visualize the interaction of molten smelt droplets falling into water, as a function of the smelt and water temperatures, smelt composition, droplet size, and the height from which the droplets fall. Results to date clearly demonstrate that droplets "explode" either at the water surface or beneath it, as long as the water temperature is below a critical value. These droplet explosions, while violent, can be very useful, as they enhance smelt dissolution. However, as the water temperature rises, the explosions become less likely, and beyond a certain temperature, droplets do not explode at all, leaving solid smelt to accumulate on the tank bottom.

INTRODUCTION

The combustion of concentrated black liquor in the recovery boiler results in the formation of molten smelt at the bottom of the boiler (Figure 1(a)), which consists of mostly Na_2CO_3 and Na_2S with small amounts of Na_2SO_4, NaCl and potassium salts [1]. Molten smelt pours out of the boiler at about 820^{o}C through one or more smelt spouts. It is shattered by a high pressure steam jet into small droplets (Figure 1(b)) before falling into the dissolving tank where it interacts with water and dissolves. The solution (green liquor) is causticized with lime in the causticizing plant to covert Na_2CO_3 into NaOH. The resulting solution, which contains mainly NaOH and Na_2S, is reused in the pulping process.

While shattering molten smelt with a high pressure steam jet, and dissolving the shattered smelt in the dissolving tank, are violent and often dangerous processes, they are necessary in order to process the large amount of molten smelt effectively, and to produce consistent green liquor. Dissolving tanks constantly rumble, and at times, cause tremors of the ground and buildings nearby. The violent smelt-water interaction can also emit a cloud of water vapor/mist that contains malodorous and toxic reduced sulfur gases around the dissolving tank area, that at times can trigger evacuation. In severe cases, explosions can occur, causing substantial equipment damage and production loss associated with unscheduled boiler downtimes. Personnel injuries and fatalities have also reportedly been caused by a tank explosion, or by being showered with hot smelt and green liquor ejected from the dissolving tank. Over the past 30 years, there has been about one explosion incident a year reported in North America [2], although the actual number could be higher as many incidents go unreported. Needless to say, one explosion incident is too many when it comes to workplace safety. As regulations on occupational health and safety have become increasingly stringent in recent years, effective and safe dissolving tank operation has become a top priority for kraft pulp mills.

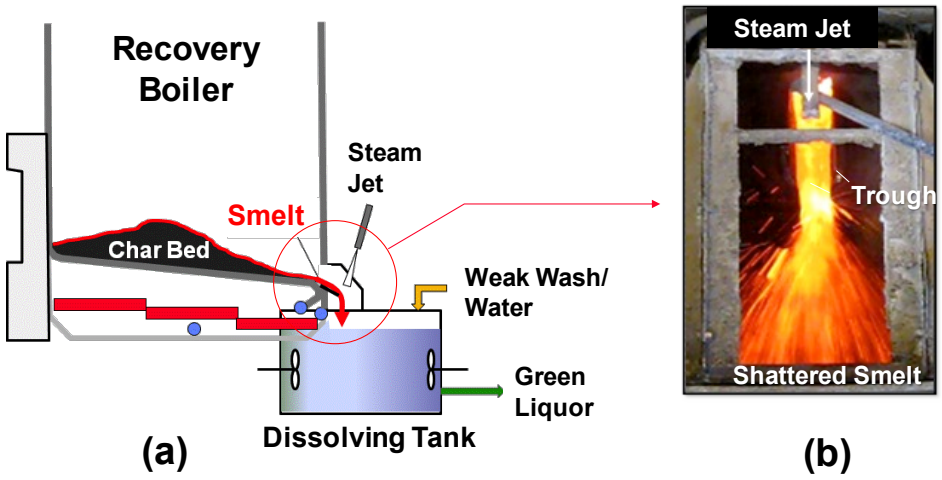

Figure 1. (a) Molten smelt stream from a recovery boiler; (b) smelt shattered by a steam jet.

Despite the importance of the problems, the triggering mechanism of a dissolving tank explosion, and the factors affecting an explosion, are not well understood. Shick and Grace [3] conducted a comprehensive literature review on liquid-liquid explosions in the early 1980's, and suggested that smelt-water explosions involve the same vapor explosion mechanism as other liquid-liquid systems, where the high heat from one liquid causes the other liquid to vaporize rapidly. However, the interaction between smelt and water in the dissolving tank differs from other liquid-liquid systems in that one liquid (molten smelt) is highly soluble in the other (water). The composition and amount of smelt dissolved are expected to have an effect on green liquor properties, and hence, on dissolving tank explosions. While liquid-liquid explosions have been intensively studied in the nuclear, metal processing, and liquefied natural gas industries [3-9], as well as in the field of oceanic volcano science [10], only two studies on smelt-water interaction in the dissolving tank environment have been published, both in the mid 1950s [11,12]. These studies were crudely carried out; the results obtained were insufficient to draw quantitative conclusions.

This paper presents an overview of two ongoing studies being conducted at the University of Toronto, on smelt shattering and dissolution. In each case we present details of the methodology and of recent results, and at the end of this paper look towards future work.

A STUDY OF SMELT SHATTERING

The study of smelt shattering was begun by Taranenko [13,14], who built an apparatus (Figure 2) to examine the shattering characteristics of water/glycerine mixtures using an air jet, as a function of air velocity, liquid viscosity, liquid flow rate and air nozzle proximity. Water is pumped from the base tank to the inclined tank and subsequently flows down a spout at a prescribed rate. An air jet nozzle is positioned above the lip of the spout to shatter the exiting water stream. Both the air and water flow rates are controlled using valves and flow meters. An optical direct imaging technique using a high speed camera captures droplet size information.

Experiments were performed using a 5/16" orifice full cone converging/diverging nozzle. The results were as expected: increasing air velocity, decreasing the liquid flow rate, and reducing the distance between the nozzle and the water stream all reduce average droplet size, as shown in Figures 3 and 4. For the range of liquid viscosities considered (1 to 50 cP), viscosity does not have a significant effect on the droplet size, unless a weak jet is used on very viscous liquid.

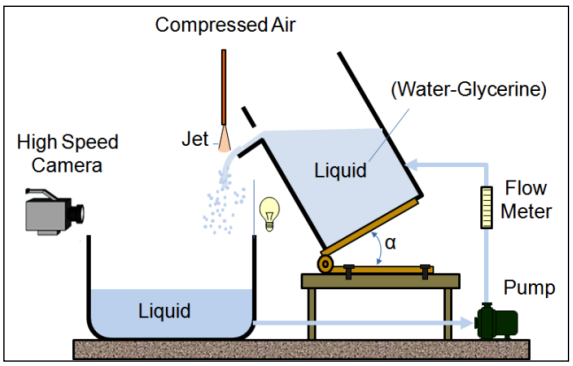

Figure 2. Lab scale shattering apparatus.

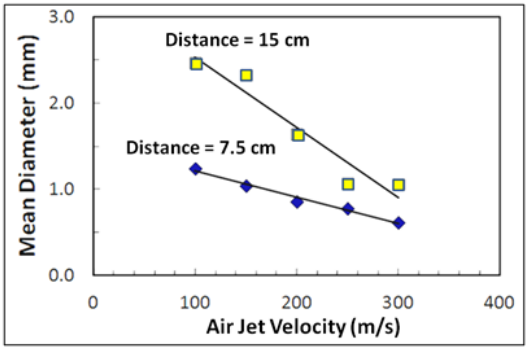

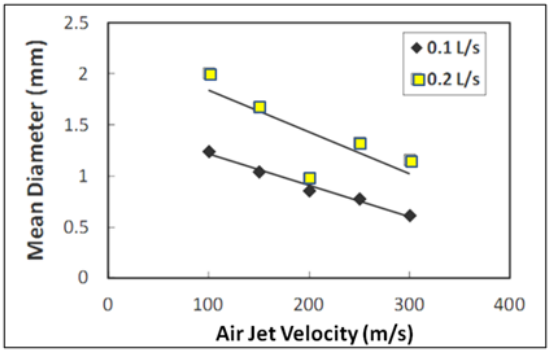

Figure 3 (left): Effect of air jet velocity and nozzle distance from the liquid stream on the Sauter Mean Diameter (SMD) of the shattered liquid. (Liquid flow rate 0.1 L/s, viscosity 2.5 cP.) **Figure 4 (right):** Effect of air velocity and liquid flow rate on SMD. (Liquid viscosity 2.5 cP, nozzle 7.5 cm from the liquid.)

Current Experimental Methodology

Recent improvements have focused on characterizing the droplet size distribution across the spray, and on automating the image analysis and processing functions. A matrix of locations is now imaged to capture a spatial distribution of droplets, and ImageJ™ image analysis software is used to process the images and calculate the projected area of droplets, information which is then used to calculate drop diameters [15]. The current study is considering the effect of different air nozzles on shattering effectiveness.

Experimental Setup

As illustrated in Figure 5, a 12 x 14 inch area two feet below the spout is imaged using a Mega-Speed™ greyscale high speed camera. Images are recorded at 42 (6 x 7) evenly spaced locations. The camera records 50 frames per second for 10 s at each location; the exposure time is 50 μs, the focal length 200 mm, and the f-stop 3.5. A light source with a diffuser is placed behind the liquid stream to provide sufficient lighting. The camera captures and stores gray scale images at 512 x 512 resolution. Only water is being used for these latest experiments, at a flow rate of 0.2 L/s. A grid system mounted above the apparatus is used to focus the camera at each imaging location.

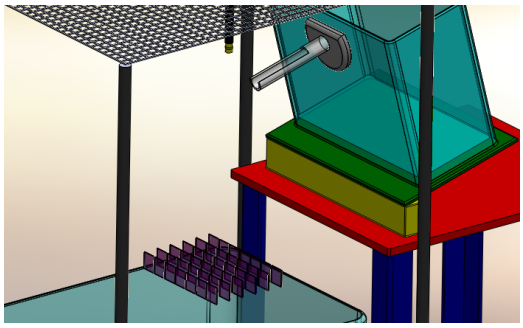

Figure 5: Schematic of the experimental setup shows the array of 42 imaging locations.

Image Analysis

Using the ImageJ software, an image analysis macro was developed to convert each grayscale image into a binary image, and filter out-of-focus droplets that cannot be accurately measured (Figure 6). The images are dimensionally calibrated and the program measures the projected area of droplets. Droplets cut off at the edges of the frame are not measured. Due to the resolution of the camera (512 x 512 pixels), it is difficult to determine if the very small droplets are in focus since they only cover a few pixels. These droplets are discounted to prevent skewing of data; therefore only droplets above 0.16 mm diameter are counted and analyzed. The average droplet projected area and count is calculated from 500 images at each of the 42 locations. Tecplot™ software is then used to plot the average droplet diameter and the droplet count distribution for each experiment, as shown in Figure 7.

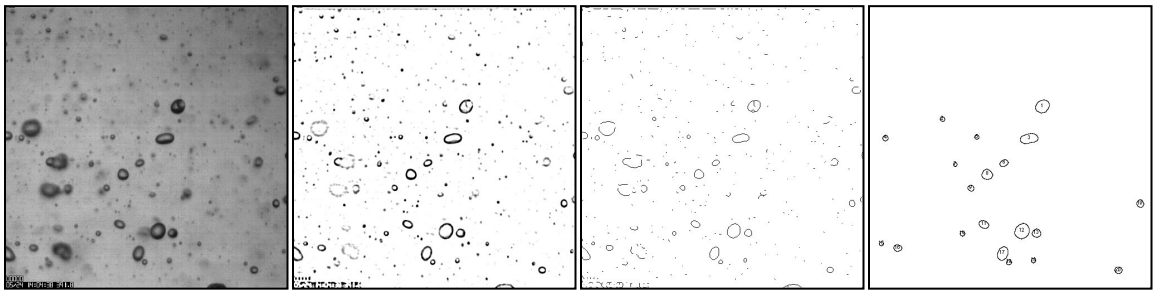

Figure 6: The series of image processes used to filter out-of-focus droplets.

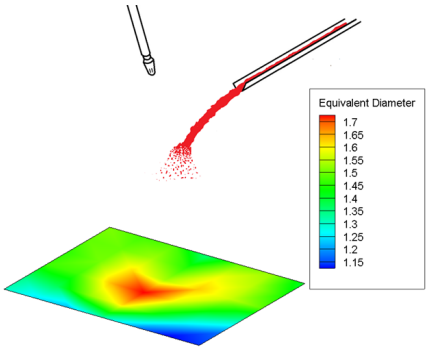

Figure 7: A sample contour illustrates average drop diameter (mm).

Research Plan

Four different lab scale nozzles are being tested, while varying the nozzle distance, orientation to the liquid stream, and the gas flow rate. The nozzle profiles are representative of nozzles in use by industry. The top of Figure 8 illustrates the four nozzles. Table 1 lists the range of each parameter.

Table 1: Experimental Parameters.

Nozzle orientation (from horizontal)	90° (vertical), 75°, 60°
Proximity to Impingement	9 inches, 7 inches, 5 inches
Air Flow Rate (standard cubic feet per minute)	10, 12.5, 15

Preliminary Results and Discussion

Figure 8 illustrates preliminary droplet size and droplet count distributions, for each of the four nozzles, at two different air flow rates, corresponding to the experimental setup illustrated in Figures 5 and 7. These experiments were conducted with the nozzle at a 90° (vertical) orientation, 7 in above the point of impingement. The spout was tilted at 15°.

The results clearly show that different nozzles produce different droplet size and count distributions. At 10 SCFM, the multi-hole thin and the flat nozzle produce generally larger droplets across a larger area than the hollow cone or the full cone nozzle. When the air jet impinges the water stream, the droplet trajectory is determined by the transfer of kinetic energy from air to water. Atomization occurs by continually shearing layers of the water stream. The top layer of the water stream receives the greatest amount of kinetic energy from the air and so is atomized more effectively, resulting in smaller droplets with higher kinetic energy scattered across a wider area. The underside of the liquid stream receives less kinetic energy from the air jet, resulting in larger droplets that retain more of their initial momentum. Both the multi-hole thin and the flat nozzle produce less shattering, so that the largest droplets (in the red zone) are further from the nozzle. This is due to the wider air distribution that these nozzles produce, which reduces the amount of air that actually impacts the water stream. The hollow cone and full cone nozzles produce smaller droplets in general, and the center of the red zone is closer to the nozzle.

Increasing the air flow rate to 15 SCFM results in a significant reduction of droplet size. For the multi-hole thin and flat nozzles, the largest droplets are closer to the nozzle, indicating a higher kinetic energy transfer from air to water. We were unable to run full cone nozzle experiments at an air flow rate of 15 SCFM.

The droplet count distributions at 10 SCFM show that the hollow and full cone nozzles produce a greater number of droplets near the nozzle, and few further from the spout. The highest droplet count is concentrated near the area with the greatest droplet diameter. When the flow rate increases to 15 SCFM, the droplet count increases significantly, because the higher air flow rate results in more effective shattering, producing smaller droplets, and more of them.

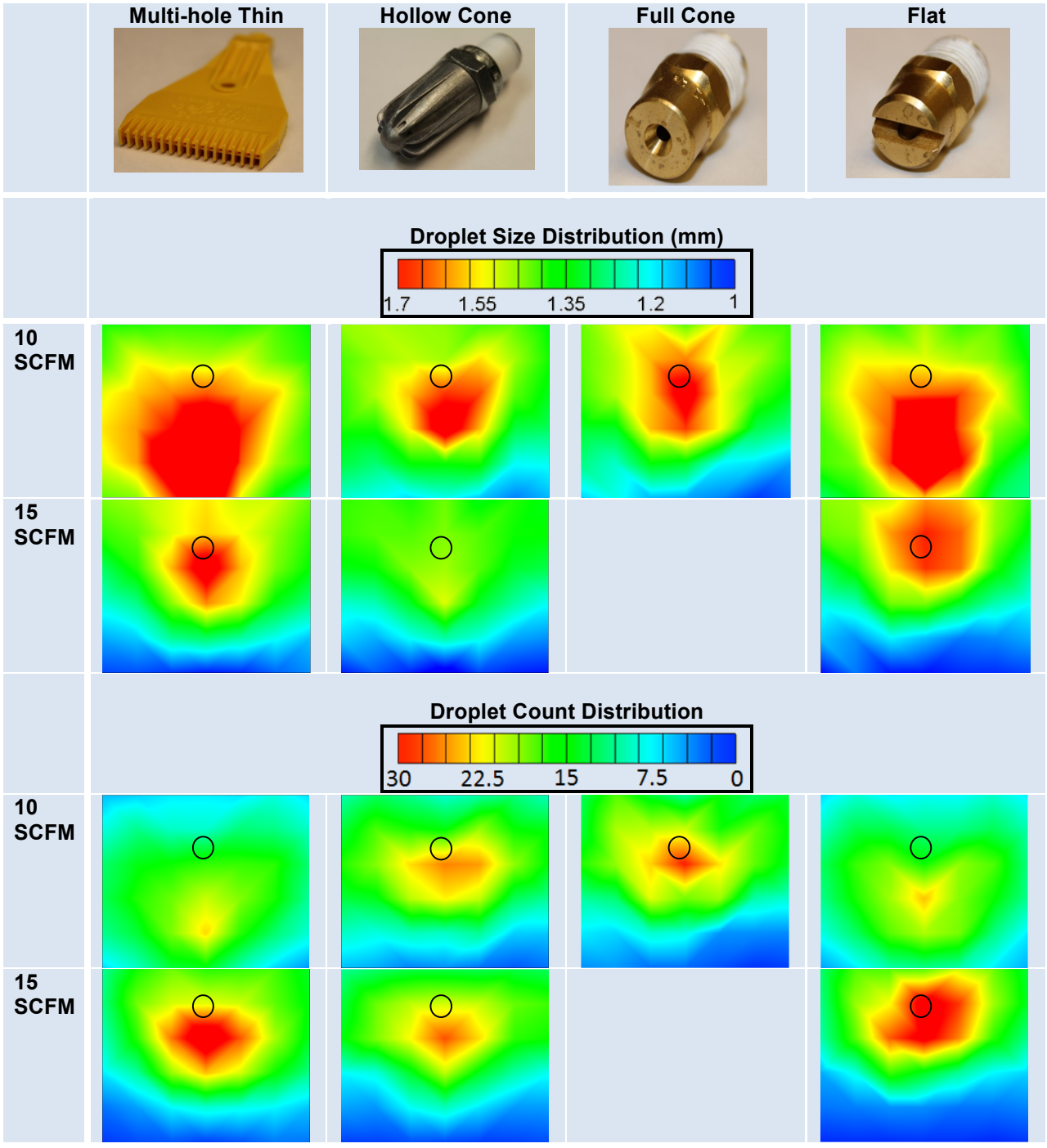

Figure 8: Droplet size and droplet count distributions over the 12 x 14 inch area two feet below the spout. The black circle represents the air nozzle location. The top of each contour is nearest the spout.

A STUDY OF SMELT/WATER INTERACTION

Our work to date on smelt/water interaction [16,17] has focused on the effects of smelt temperature and water temperature on the behaviour of droplets falling into water. Here we review some of those results, and look ahead to future research.

Experimental Setup

The synthetic smelt used in this study was a mixture of 80wt% Na_2CO_3 and 20wt% NaCl powder. This composition was chosen because the sample has a complete melting temperature of 750°C, and so would be completely molten in the crucible at the temperatures examined. A schematic of the experimental apparatus used in the study of smelt-water interaction is shown in Figure 9.

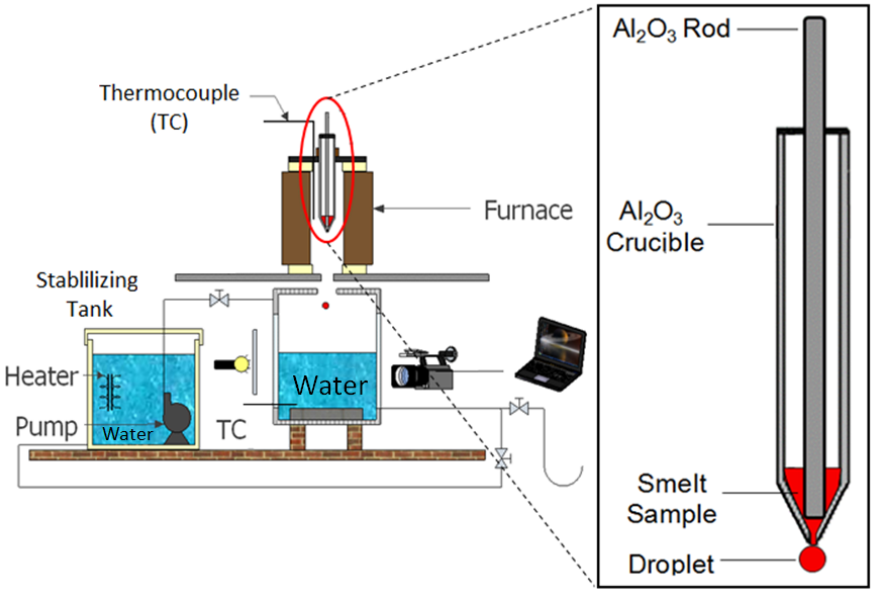

Figure 9: Experimental apparatus for the smelt-water interaction experiments.

A 220 mm long cast alumina (Al_2O_3) tube crucible with a 30 mm ID open top end and a 3 mm ID hole at the tapered bottom end is housed in a tubular electric furnace. A cast Al_2O_3 rod is inserted vertically into the crucible from the top, to loosely seal the hole at the tapered bottom end. Pulverized synthetic smelt is fed into the crucible from the top and accumulates at the bottom, in the space between the crucible and the rod. As the crucible is heated up in the furnace to the desired temperature, molten smelt begins to seep out from the crucible through the rod seal, and a droplet eventually falls out of the crucible from the bottom hole.

A 22 liter rectangular main tank is located beneath the furnace. It consists of stainless steel side walls and transparent polycarbonate front and back walls so that the behavior of smelt droplets can be observed. Water is heated in a 40 liter stabilizing tank using a temperature-controlled coiled heater, and circulated between the two tanks through a submersible pump. A video camera with a frame rate of 25 frames per second is placed in front of the tank to record the behavior of each smelt droplet as it falls into the tank and interacts with water. Two light bulbs and a diffuser are mounted behind the back wall of the tank to illuminate the experiment. A computer connected to the video camera allows for real-time monitoring of smelt-water interactions in the water tank, and the storage of video data.

In this study, the size of the droplets was around 7 mm, measured by comparing video images with a calibrated image. The droplets fell about 700 mm, and the water level in the tank was 120 mm. Experiments were carried out at three smelt temperatures (T_s): 800°C, 900°C and 1000°C, and the water

temperature (T_w) was varied between 25°C and 100°C. For each condition, at least 30 droplets were generated.

Results and Discussion

The behavior of a molten smelt droplet in water depends on the smelt temperature and water temperature. Series of photos recorded by the video camera show three distinct interactions, shown in Figure 10. Some droplets break into small pieces upon contact with the water and disintegrate immediately at the water surface (*Immediate Explosion*). Some sink beneath the water surface and explode either in the middle of the water tank or after settling on the tank floor (*Delayed Explosion*). Finally, some droplets sink to the bottom of the tank and solidify without exploding (*No Explosion*). To quantify the effects of T_s and T_w on the interaction, the "explosion probability" and "explosion delay time" (dt) were investigated.

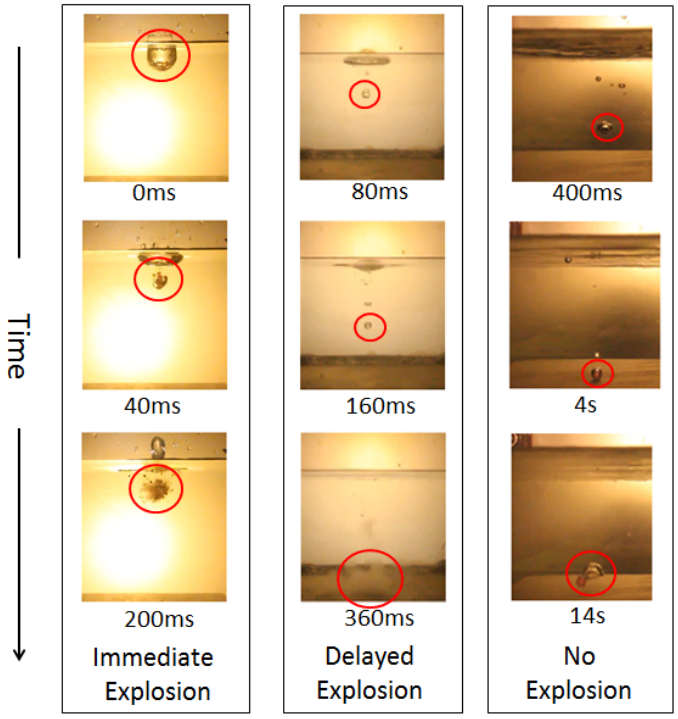

Figure 10: Three regimes of smelt-water interaction (the red circles highlight the droplets).

The probability of explosion was calculated by dividing the number of droplets that exploded by the total number of droplets tested for each experimental condition (about 30). As shown in Figure 11, at a given T_s there is a water temperature range below which the explosion probability is 100% (i.e. droplets always explode) and above which the explosion probability is 0% (i.e. no droplets explode). We define the low end of this temperature range as the lower critical water temperature, Lower $T_{crit,w}$, and the high end as the upper critical water temperature, Upper $T_{crit,w}$. The results clearly show that the Lower $T_{crit,w}$ decreases with increasing smelt temperature: 72°C for T_s= 800°C, 65°C for T_s= 900°C and 50°C for T_s=1000°C. The Upper $T_{crit,w}$, on the other hand, remains the same at 82°C for all cases. The explosion probability for a real kraft smelt sample at 800°C was also tested, and it was found to follow the same pattern as the synthetic smelt.

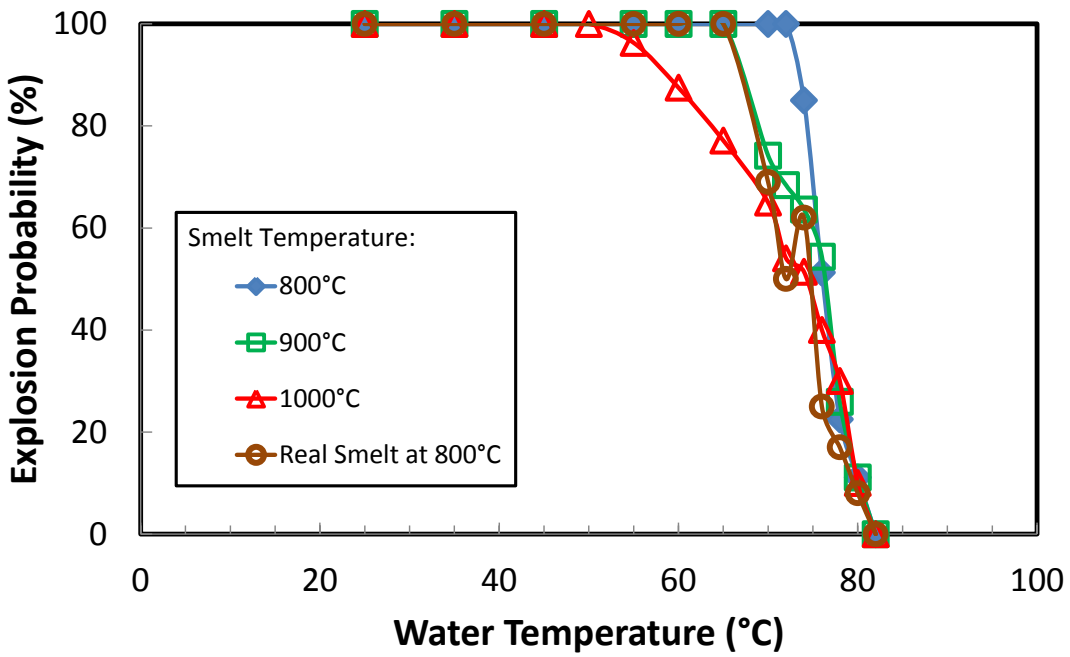

Figure 11: Explosion probability at different water (T_w) and smelt (T_s) temperatures.

The data in Figure 11 can be presented to show the combined effect of T_s and T_w on the explosion probability of molten synthetic smelt droplets; we call this a Smelt-Water Interaction Temperature (SWIT) diagram, Figure 12. The diagram predicts how molten smelt and water interact at different temperatures. Below the Lower $T_{crit,w}$ curve, droplets always explode. Above the Upper $T_{crit,w}$ line at 82°C, no droplets explode. Between the lower and upper critical water temperatures, a droplet may or may not explode. The left boundary of the SWIT diagram is the freezing temperature of the synthetic smelt, 750°C, although it may be possible that droplets can explode at lower temperatures if supercooled or only partially frozen.

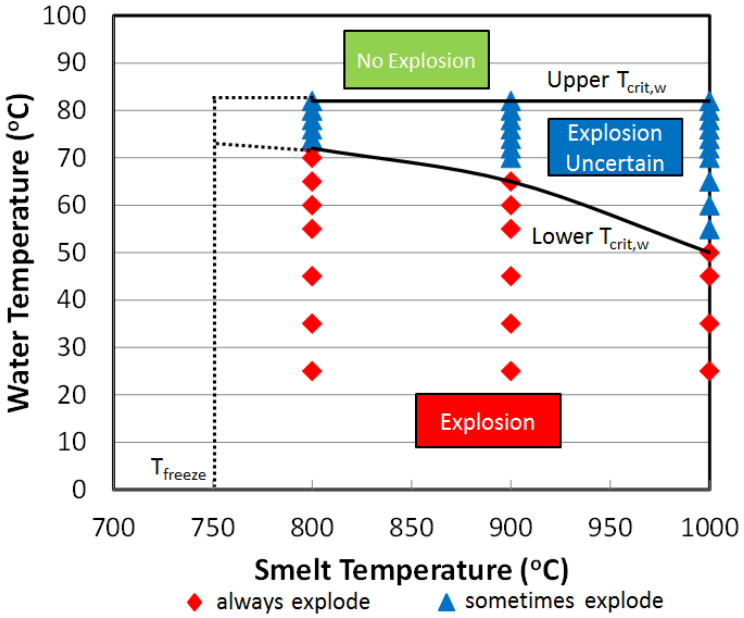

Figure 12: Smelt-Water Interaction Temperature (SWIT) diagram (80% Na_2CO_3 and 20% NaCl).

We define the explosion delay time (dt) as the duration between first contact with water and when a droplet explodes. The contact time was determined from the video recordings, and the explosion time was obtained from the acoustic signal recorded by the camera. Figure 13 illustrates the droplet explosion delay time at different smelt and water temperatures. At a given T_s, dt increases with increasing T_w; dt also increases as T_s increases.

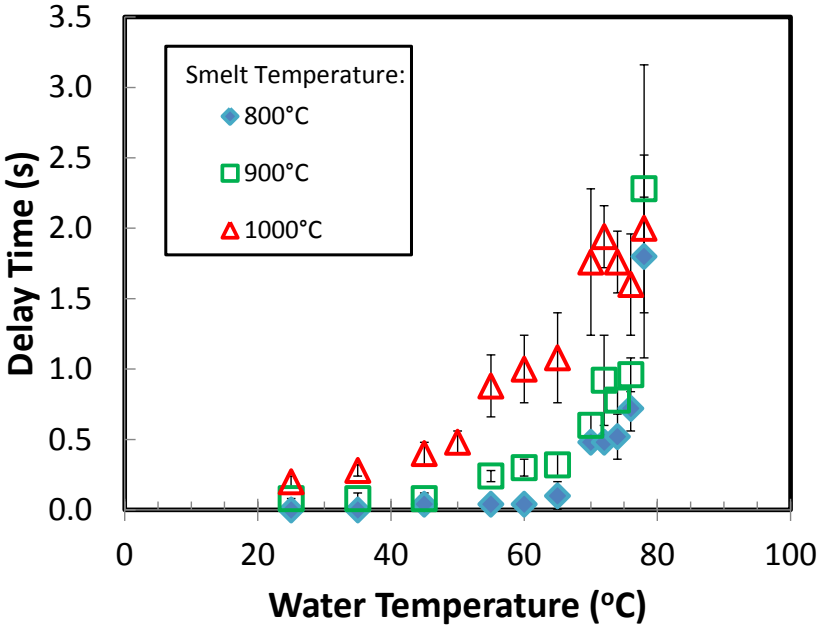

Figure 13: Droplet explosion delay time (dt) at different smelt (T_s) and water (T_w) temperatures.

The explosion delay time offers insight on the effect of the tank bottom on the droplet behavior. With 120 mm of water in the tank, droplets take about 0.4 s to impact the tank bottom for the first time; if they bounce and don't explode, the second impact usually occurs at dt=0.8 s. Figure 14 superimposes the data of Figures 11 and 13: explosion probability and delay time at different T_w. Notice that the delay time curves plateau at about 0.4 s for all three smelt temperatures, and towards the end of each plateau, the corresponding explosion probability begins to decrease. This suggests that the impact on the tank bottom can trigger some droplet explosions, and that it is only an incremental rise in T_w that can overcome the effect of the tank bottom, so that dt begins to rise again. The droplets that survive the first impact may not explode. The second plateau appears at dt = 0.8 s for T_s=900°C and 1000°C, and corresponds to droplets that survived the first impact, bounced up, and impacted the tank bottom a second time. In a sense, the existence of the tank bottom shifts the explosion probability curve upwards. The delay time asymptotes towards infinity when the upper $T_{crit,w}$ is reached, and the smelt droplets no longer explode. The data is more scattered as the delay time increases, reflecting the stochastic nature of smelt explosions, and/or the low probability of explosions at high water temperature.

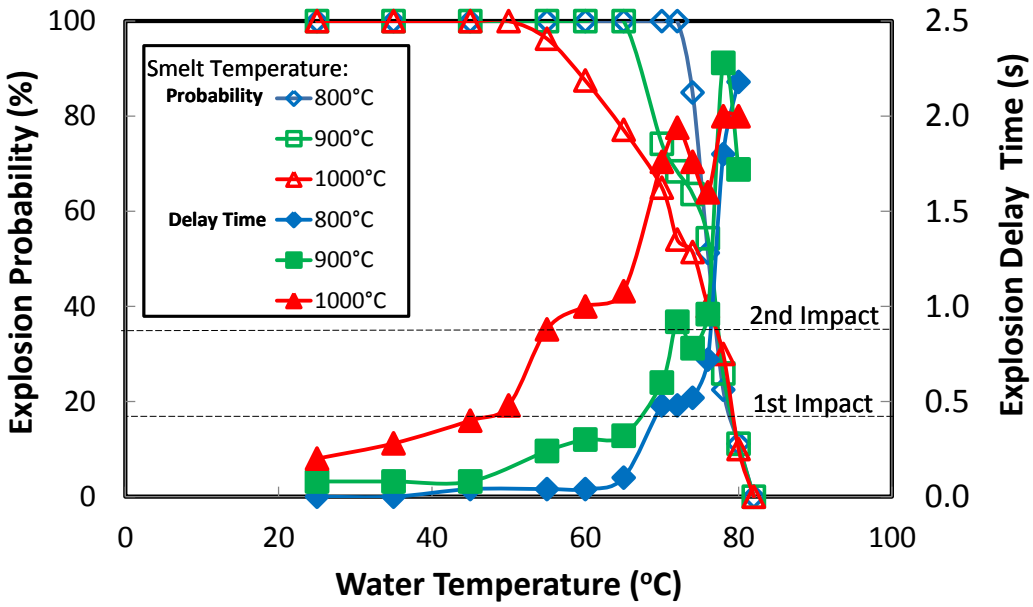

Figure 14: Explosion probability (left) and delay time (right) at different smelt and water temperatures.

FUTURE WORK

These initial studies offer insights into how molten smelt is shattered by a steam jet, and how a molten smelt droplet behaves in water, yet there are many questions that must be addressed before meaningful conclusions can be drawn. Our work on assessing different shatter jet nozzle profiles will continue, as we try to identify nozzles that shatter better than others, or that shatter as effectively as others while using less air (i.e. steam). Additional experiments will be conducted to look at droplet size distributions on other planes beneath the spout, to predict the spray growth pattern. We plan to correlate droplet size distributions to appropriate non-dimensional parameters, in order to extrapolate experimental results to predict droplet size distributions at mill scale. Questions for future research include: How does shatter jet nozzle placement, relative to the spout, affect shattering? And how well can we expect to shatter so-called "jelly roll smelt", that is very viscous?

The experimental work on smelt/water interaction will also continue. The experimental apparatus is currently being rebuilt to allow us to vary parameters including smelt droplet size, smelt composition, green liquor concentration, and the distance droplets fall before reaching the tank. Acoustic and vibration data will be collected to analyze the intensity of droplet explosions. Questions for future research include: How does the explosion probability vary with smelt droplet size and distribution? Does partially molten smelt explode? Does the distance between the smelt spout and liquor level in the dissolving tank affect the tendency for immediate explosions? How does one exploding droplet affect the tendency for other droplets to explode? Can we quantify synergetic effects between exploding droplets? How do green liquor composition and concentration affect the tendency for droplets to explode? How can our lab-scale results be applied to mill conditions?

ACKNOWLEDGEMENTS

This work was conducted as part of the research program on "Increasing Energy and Chemical Recovery Efficiency in the Kraft Process - III", jointly supported by the Natural Sciences and Engineering Research Council of Canada (NSERC) and a consortium of the following companies: Andritz, AV Nackawic, Babcock & Wilcox, Boise, Carter Holt Harvey, Celulose Nipo-Brasileira, Clyde-Bergemann, DMI Peace River Pulp, Eldorado, ERCO Worldwide, Fibria, FP Innovations, International Paper, Irving Pulp & Paper, Kiln Flame Systems, Klabin, MeadWestvaco, Metso Power, StoraEnso Research, Suzano, Tembec and Tolko Industries.

REFERENCES

1. Grace T.M., "Chapter 11 - Recovery Boiler Safety", in Kraft Recovery Boilers, T.N. Adams, Editor, TAPPI Press, Atlanta, p. 333 (1997).
2. Lien S. and DeMartini N. "Dissolving Tank Explosions: A Review of Incidents between 1973 and 2008". Unpublished report to BLRBAC and AF&PA, sponsored by the American Forest & Paper Association, New York (2008).
3. Shick P.E. and Grace T.M. "Review of smelt water explosions", Proceedings of the International Chemical Recovery Conference, p. 155-164, Sponsored by the Technical Section of CPPA and TAPPI, Vancouver, September 22-25, 1981.
4. Dullforce T.A., Buchanan D.J. and Peckover R.S., "Self-triggering of small scale fuel-coolant interaction: I. Experiments", Journal of Physics D: Applied Physics, 9: 1295-1303 (1976).
5. Buchanan D.J. and Dullforce T.A., "Mechanism of vapor explosions", Nature, 245, 32-34 (1973).
6. Reid R.C., "Rapid phase transitions from liquid to vapour", Advances in Chemical Engineering, 12, 105-208, (1983).
7. Epstein S.G., "Molten Aluminum-Water Explosions: An Update", In Light Metals 1993 (S. K. Das, ed.), Metallurgical Society of AIME, 845-853 (1992).
8. Katz D.L. and Sliepcevich C.M., "Liquefied Natural Gas/Water Explosions: Cause and Effect", Hydrocarbon Process, 50, 240-244 (1971).
9. Corradini M.L., Kim B.J. and Oh M.D., "Vapor explosions in light water reactors: A review of theory and modeling", Progress in Nuclear Energy, 22(1), 1-117 (1988).
10. Francis P. and Self S. "The Eruption of Krakatau", Scientific American, 249, 149-159 (1983).
11. Sallack J.A., "An investigation of explosions in the soda smelt dissolving operation", Pulp Paper Canada Magazine, 56(10): 114-118 (1955).
12. Nelson W. and Kennedy E.H., "What causes kraft dissolving tank explosions, I. Laboratory Experiments", Paper Trade Journal, 140(29): 50-56 (1956).
13. Taranenko A., "Shattering Recovery Boiler Smelt by a Steam Jet", M.A.Sc. thesis, University of Toronto (2012).
14. Taranenko A., Bussmann M. and Tran H.N., "A laboratory study of recovery boiler smelt shattering," Proceedings of TAPPI PEERS, Green Bay, WI (2013).
15. ImageJ, developed at the National Institutes of Health, available at www.imagej.net.
16. Jin E., "Interaction between a Molten Smelt Droplet and Water", M.A.Sc. thesis, University of Toronto (2013).
17. Jin E., Bussmann M. and Tran H.N., "An experimental study of smelt-water interaction in the recovery boiler dissolving tank," Proceedings of TAPPI PEERS, Green Bay, WI (2013).